Channel Estimation for FBMC/OQAM with Fast Fading Channels by Kalman Filter

Shaochuan Wu, Xiaoqing Liu,Yuming Wei, Xu Bai
School of Electronics and Information Engineering
Harbin Institute of Technology
Harbin, China
scwu@hit.edu.cn, liuxiaoqing0608@163.com,14b905018@hit.edu.cn, 77454053@qq.com

***Abstract*—Since offset QAM-based filter bank multicarrier (FBMC/OQAM) systems has inherent imaginary interference, most channel estimation techniques for FBMC are now scattered auxiliary pilots on slow-fading channels. However, in more demanding scenarios, auxiliary pilots can prove to cause serious mistakes. In this paper, an algorithm of Kalman filter channel estimation based on feedback interference calculation pilot in fast fading channels is proposed. Simulation results show that the proposed method has good performance in time-varying multipath channels. Compared with the traditional channel estimation methods, the proposed method has greatly improved its performance.**

***Index Terms*—Filter-Bank Multi-Carrier, Offset Quadrature Amplitude Modulation, Channel Estimation, Kalman Filter**

I. Introduction

Orthogonal Frequency Division Multiplexing (OFDM) technology is known for its robustness against multipath time-varying transmission channels and is widely used in modern wireless communication networks. However, with the development of the times, the demand of users for the rate and capacity of data transmission in communication systems is on the rise. How to maximize the use of spectrum resources under the existing limited spectrum resources and into depletion has become an urgent need in modern communication systems one of the problems solved. Compared with OFDM technology nowadays, FBMC technology shows excellent performance both in spectrum utilization and spectrum leakage. It is for these reasons that FBMC technology has become the future alternative OFDM technology as an optional 5G physical layer technology program[1].

FBMC/OQAM not only provides spectrum efficiency similar to that of OFDM without cyclic prefix, but also introduces a filter with good time-frequency focusing characteristics due to the relaxation of orthogonal conditions, which makes the system have good anti-interference ability. In addition, the FBMC/OQAM system has a strong analogy with OFDM in principle[2]. Therefore, most mature technologies of OFDM can be transplanted to FBMC/OQAM. In fact, in FMBC/OQAM system, the imaginary inherent interference exists in the complex number domain because adjacent filters only satisfy the orthogonal in the real domain. Then the channel estimation method used in OFDM system is no longer applicable in FBMC/OQAM system[3]. Since the channel estimation can accurately analyze the channel state, the insertion position of the pilot channel will affect the channel estimation effect to a certain extent, thus affecting the transmission performance of the system. Therefore, in order to accurately obtain the channel estimation at the pilot position, a scheme to resist inherent interference needs to be considered to eliminate the influence of inherent interference on the pilot as much as possible[4].

In[5–8], different schemes have been designed for scattered pilots to eliminate the pilot interference. A new concept of Auxiliary Pilot (AP) was introduced to eliminate interference at pilot positions in [5]. By doing this, the received primary pilot becomes non-interfering and the channel estimation can be performed in the same manner as the OFDM system. [6] is based on the idea of using some AP symbols to eliminate virtual interference on each scattered pilot. AP symbols are encoded to carry information symbols in order to keep spectral efficiency of transmission high. [7] proposed a semiconductor channel estimation approach that provides improved power efficiency by grouping the pilot signals and applying symbol ambiguity to them compared to the auxiliary pilot method in [5].

The existing channel estimation algorithms mostly assume that the channel is quasi-static, that is, the channel impulse response is basically unchanged or changes slowly within an FBMC symbol time, and can be neglected approximately. However, under high-speed mobile environment, the Doppler shift will lead to the change of channel impulse response in a short time, making the system a time-varying system. The existence of Doppler frequency shift on the wireless channel makes the channel characteristics time-variant, which brings difficulties to the channel estimation.

Kalman filter technology is a method that can be used to estimate the state of a system online. The state vector of the system is reconstructed from the measured values and recursively estimated in the order of 'Predicted - Measured - Modified' to eliminate random interference and then reproduce the status of the system. Kalman filter uses the state equation to describe the dynamic changes of state variables, it does not need to know all the past values, so it is more suitable for time-varying systems.

This paper proposes a Kalman filter channel estimation algorithm based on feedback interference calculation pilot[9] in fast fading channel. According to the channel related

978-1-5386-2070-0/18/$31.00 ©2018 IEEE

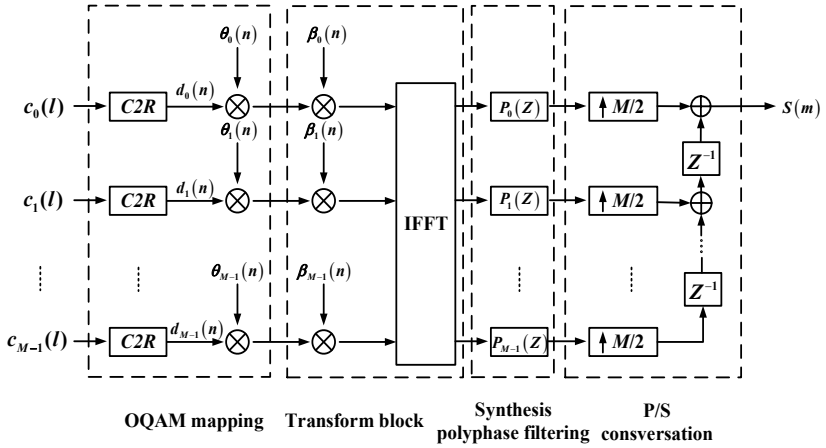

Fig. 1. Block diagram of the FBMC/OQAM transmitter

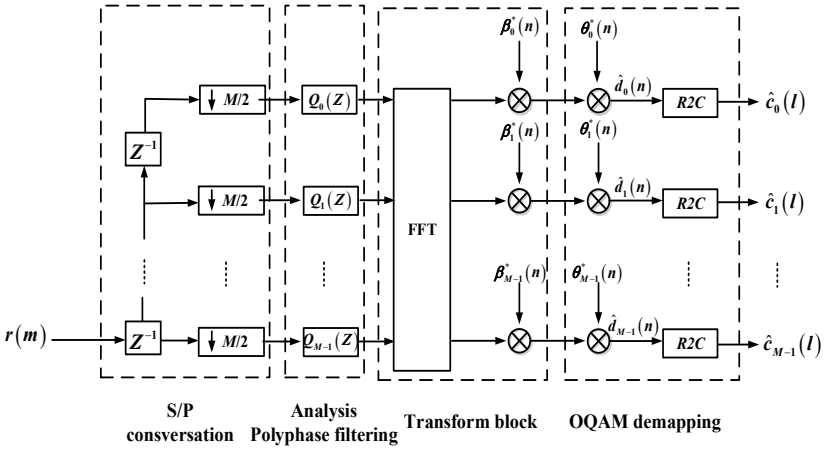

Fig. 2. Block diagram of the FBMC/OQAM receiver

changes, the use of Kalman filtering method for channel tracking. Adopting the pilot based on feedback interference calculation will reduce the error when Kalman filtering tracks the channel by using FBMC internal interference, which will help Kalman filtering to track the channel more accurately. Simulation results show that the Kalman filtering channel estimation algorithm based on feedback calculation pilot which is proposed this paper has good performance and is suitable for time-varying systems with high-speed mobile.

The paper is organized as follows. In Section II, the conventional FBMC/OQAM system is introduced. Section III presents the proposed Kalman filter channel estimation algorithm based on feedback interference pilot for channel estimation of FBMC. Simulation results are presented in Section IV. Section V concludes this paper.

II. FBMC/OQAM COMMUNICATION SYSTEM

The generalized block diagram of the FBMC/OQAM transmitter and receiver are illustrated in Fig.1 and Fig.2.

In the Fig.1, $c_k\,(l)$ represents the complex symbol after the process of QAM constellation mapping, and $C2R$ represents the transformation of a complex to real. $d_k\,(n)$ denotes the real-value data symbol mapped onto the kth subcarrier and the nth FBMC/OQAM symbol, transmitted at a rate of $2/T$ where the signaling period is defined as $T = 1/\Delta f$ with Δf being the subcarrier spacing. For the sake of simplicity, $d_k\,(n)$ is denoted as $d_{k,n}$. With M subcarriers, the transmit signal of the FBMC/OQAM system can be represented as

$$s\,(m) = \sum_{k=0}^{M-1} \sum_{n=-\infty}^{\infty} d_{k,n}\theta_k\,(n)\,g\left(m - \tfrac{nM}{2}\right)\varepsilon_k\,(m) \qquad (1)$$

where $g\,(m)$ stands for the impulse response of the prototype filter and the length of the prototype filter is L_p. A phase rotation $\theta_k\,(n) = j^{k+n}$ is applied in order to map $d_{k,n}$ into the real and imaginary domains alternatively in the time-frequency grid and

TABLE I
INTERFERENCE FACTOR OF PHYDYAS FILTER $K = 4$

f \ t	-4	-3	-2	-1	0	1	2	3	4
-2	0	0.0006	-0.0001	0	0	0	-0.0001	0.0006	0
-1	0.0054	0.0429j	-0.125	-0.2058j	0.2393	0.2058j	-0.125	-0.0429j	0.0054
0	0	-0.0668	0.0002	0.5644	1	0.5644	0.0002	-0.0668	0
1	0.0054	-0.0429j	-0.125	0.2058j	0.2393	-0.2058j	-0.125	0.0429j	0.0054
2	0	0.0006	-0.0001	0	0	0	-0.0001	0.0006	0

$$\begin{aligned}\varepsilon_k(m) &= (-1)^{kn} e^{-j\frac{2\pi k}{M}\left(\frac{L_p-1}{2}\right)} \mathrm{e}^{j\frac{2\pi km}{M}} \\ &= \beta_k \gamma_k(m)\end{aligned} \tag{2}$$

where

$$\gamma_k(m) = \mathrm{e}^{j\frac{2\pi km}{M}} \tag{3}$$

$$\beta_k = (-1)^{kn} e^{-j\frac{2\pi k}{M}\left(\frac{L_p-1}{2}\right)} \tag{4}$$

The prototype filter $g(m)$ is well-localized in time and/or frequency domains, and satisfies the real-orthogonality defined as[10].

$$\Re\left\{\langle g_{k,n}|g_{p,q}\rangle\right\} = \Re\left\{\int g_{k,n}(m)\, g^*_{p,q}(m)\right\} = \delta_{k,p}\delta_{n,q} \tag{5}$$

where $\delta_{p,q}$ denotes the Kronecker delta function. Filter banks satisfying (5) are called perfect-reconstruction (PR) filter banks. In practice, nearly perfect-reconstruction (NPR) designs are sufficient, because they provide a higher stopband attenuation than their equal-length PR counterparts while the cross-talk between subchannels is small enough to be ignored. In this paper, we take PHYDYAS prototype filter[11] as NPR prototype filter. The length L_p of the prototype filter $g(m)$ depends on the size of the filter bank and the number of FBMC/OQAM symbol waveforms K that overlap in time as $L_p = KM$. The finite impulse response (FIR) of the low-pass prototype filter can be expressed as

$$g(m) = 1 + 2\sum_{k=1}^{K-1} G_k \cos\left(2\pi\frac{km}{KT}\right) \tag{6}$$

where G_k are the filter coefficients, satisfying the following conditions.

$$\begin{cases} G_0 = 1 \\ G_k^2 + G_{K-k}^2 = 1; G_{L_p-k} = G_k; 1 \le k \le K-1 \\ G_k = 0; K \le k \le L_p - K \end{cases} \tag{7}$$

The frequency response of the PHYDYAS prototype filter is as shown in Fig.3.

Because of a lack of the orthogonality in the complex domain, even in the absence of the channel fading, noise, and synchronization mismatch, there always exist purely imaginary intercarrier and intersymbol interferences at the output of the analysis filter bank (AFB). It is summarized in Table I considering the PHYDYAS filter with the overlapping factor of 4.

As shown in Fig.2, the receiver is the reverse process of the transmitter. The multiplicative factors $\theta_k(n)$ and $\beta_k(n)$ corresponding to the transmitter at the receiver become their conjugate $\theta_k^*(n)$ and $\beta_k^*(n)$.

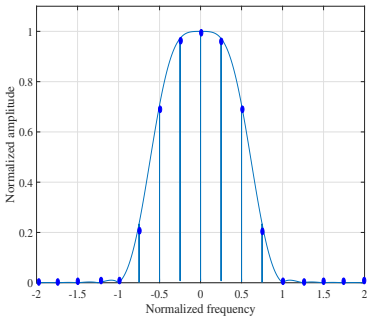

Fig. 3. The frequency response of the prototype filter $K = 4$

III. FBMC/OQAM PILOT ARRANGEMENT AND KALMAN FILTER

The transmitted FBMC/OQAM signal $s(m)$ in (1) is assumed to go through a time-varying frequency-selective Rayleigh fading channel with background additive white Gaussian noise (AWGN). Assuming that the allocated bandwidth for each subcarrier is less than the coherence bandwidth of the wireless channel, each subcarrier undergoes frequency nonselective flat-fading. Thus, the received signal can be expressed as

$$y(t) = \sum_{n=-\infty}^{\infty}\sum_{k=0}^{M-1} h_{k,n} d_{k,n} g_{k,n}(t) + n(t) \tag{8}$$

where $n(t)$ represents channel additive noise of a variance N_0, $h_{k,n}$ denotes the channel frequency response at the kth subcarrier and a time instance n.

In order to detect d_{k_0,n_0} , a matched filtering needs to be performed. The output of the matched filter is given by

$$\begin{aligned} r_{k_0,n_0} &= \int y(t) g^*_{k_0,n_0}(t)dt \\ &= h_{k_0,n_0}\left(d_{k_0,n_0} + j\sum_{(p,q)\neq(0,0)} u^{k_0,n_0}_{k_0+p,n_0+q}\right) \\ &\quad + \tilde{n}_{k_0,n_0} \\ &= h_{k_0,n_0}\left(d_{k_0,n_0} + j\sum_{(p,q)\neq(0,0)} t^{k_0,n_0}_{k_0+p,n_0+q} d_{k_0+p,n_0+q}\right) \\ &\quad + \tilde{n}_{k_0,n_0} \\ &= h_{k_0,n_0}\left(d_{k_0,n_0} + j u_{k_0,n_0}\right) + \tilde{n}_{k_0,n_0} \end{aligned} \tag{9}$$

where $ju_{k_0+p,n_0+q}^{k_0,n_0}$ is the intrinsic interference induced from the (k_0+p)th subcarrier of (n_0+q)th symbol to the k_0th subcarrier of n_0th symbol , $t_{k_0+p,n_0+q}^{k_0,n_0}$ is interference weights in Table I, $\tilde{n}_{k_0,n_0}$ is the effective noise at the output of AFB and its variance is N_0, which is expressed as

$$\tilde{n}_{k_0,n_0} = \int n(t) g_{k_0,n_0}^{*}(t) dt \tag{10}$$

It is obvious that the real value extraction after channel equilibrium can successfully suppress the imaginary-value inherent interference ju_{k_0,n_0} in (9). For example, the output signal of a zero-forcing equalizer becomes

$$\Re\left\{r_{k_0,n_0}/h_{k_0,n_0}\right\} = d_{k_0,n_0} + \Re\left\{\tilde{n}_{k_0,n_0}/h_{k_0,n_0}\right\} \tag{11}$$

from which d_{k_0,n_0} can be recovered undisturbed. In the aspect of symbol recovery, as described in (11), imaginary-value interference can be processed at the receiver. However, in channel estimation aspects, due to the intrinsic interference is a zero-mean gaussian random variable with variance of $\sigma^2 = E\left[|d_{k,n}|^2\right]$ [10], this process cannot be realized.

$(d_{k,n} + ju_{k,n})$ is represented by $x_{k,n}$, then the receive signal on the kth subcarrier of nth symbol can be expressed as

$$r_{k,n} = h_{k,n} x_{k,n} + \tilde{n}_{k,n} \tag{12}$$

The high relative velocity of the transmitter and the receiver will lead to a large Doppler frequency, resulting in a rapid change in the channel, i.e. the Channel response is different on different symbols of the same subcarrier. The higher the Doppler frequency is, the faster the change is. In general, a comb-based pilot-based channel estimation algorithm will be used to cope with the drastic changes of this channel. Although the comb pilot can track the channel changes well, the comb pilot can not get the true channel response due to the imaginary part interference in FBMC/OQAM. So it is using comb pilot based on auxiliary pilot arrangement[9] as shown in Fig.4.

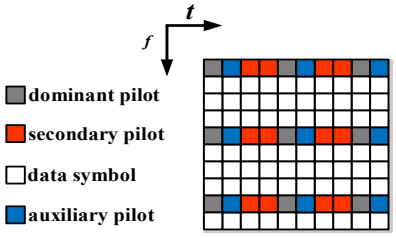

Fig. 4. A comb pilot based on auxiliary pilot

As shown in Fig.4, the pilot with the auxiliary pilot is called dominant pilot. The secondary pilot does not have auxiliary pilot to help it eliminate interference. The auxiliary pilot is calculated as

$$d_{k_a,n_a} = -\frac{\sum_{(k,n)} d_{k,n} t_{k+p,n+q}^{k,n}}{t_{k+p,n+q}^{k,n}} \tag{13}$$

where $(k,n) \in \Omega_{k_p,n_p}, (k,n) \neq (k_a,n_a), (k,n) \neq (k_p,n_p)$, d_{k_a,n_a} represents the auxiliary pilot at the position (k_a,n_a), and $t_{k+p,n+q}^{k,n}$ is interference weights in Table I, Ω_{k_p,n_p} is a window for calculating the auxiliary pilot. The feedback interference calculation method is used to calculate the interference of the secondary pilot position, the algorithm flow chart is shown in Fig.5.

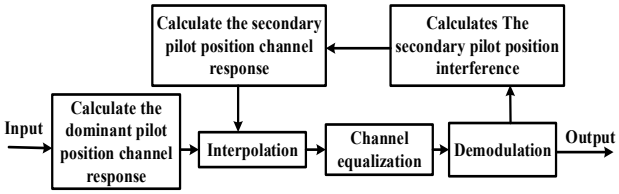

Fig. 5. Feedback interference calculation algorithm

The feedback interference calculation algorithm first uses the pilot information with auxiliary pilot to estimate and interpolate the information of the entire channel, obtains the estimation of the transmitted signal through equalization and demodulation, and then calculates the interference information of the pilot position by using the estimated transmitted signal, that is, by using the estimated symbols around the demodulated pilot symbols and the interference coefficients in Table I, the imaginary interferences on the pilot symbols are calculated, thus can get $(d_{k,n} + ju_{k,n})$, which is $x_{k,n}$.

The statistical characteristics of the channel fading process are given by the power spectral density and the autocorrelation function. The channel response power spectral density is the U-band limited spectrum.

$$S(f) = \begin{cases} \frac{1}{\pi f_d \sqrt{1-(f/f_d)^2}}, & |f| \leq f_d \\ 0, & elsewhere \end{cases} \tag{14}$$

where f_d is maximum Doppler frequency. The autocorrelation function of the channel response can be written as the first-order zero-order Bessel function.

$$R(k) = J_0\left(2\pi f_d T |k|\right) \tag{15}$$

Any stationary random process can be represented as an infinite order AR process. This property enables the fading channel to be expressed in the form of an AR process[12].

$$h_n(k) = \sum_{i=1}^{p} a_i h_{n-i}(k) + v_n(k) \tag{16}$$

where p and a_i are the order and the coefficient of the AR process, respectively. $v_n(k)$ is a white Gaussian noise with zero mean and variance σ_v^2. The choice of p represents the tradeoff between the accuracy of the model (16) and the difficulty in estimating its parameters. In this paper, in order not to increase the computational complexity, only the first order AR model, i.e. $p = 1$, is considered. Then, assuming that the process of each tap-gain for the fading channel paths is independent and identically distributed (i.i.d.), the vector form of the channel is obtained as follows.

$$\mathbf{h}_n = \mathbf{F}_n \mathbf{h}_{n-1} + \mathbf{v}_n \tag{17}$$

where $\mathbf{h}_n = [h_n \quad h_{n-1} \quad \cdots \quad h_{n-p+1}]^T$,

$$\mathbf{F_n} = \begin{bmatrix} a_1 & a_2 & \cdots & a_p \\ 1 & 0 & \cdots & 0 \\ \vdots & \vdots & \ddots & \vdots \\ 0 & \cdots & 1 & 0 \end{bmatrix}.$$

Combining this model of (17) with (12), it can be obtained the following state-space model on the kth subcarrier.

$$\begin{aligned} \mathbf{h}_{n+1} &= \mathbf{F}_n \mathbf{h}_n + \mathbf{v}_{n+1} \\ r_n &= \mathbf{x}_n^T \mathbf{h}_n + \tilde{n}_n \end{aligned} \tag{18}$$

where $\mathbf{x}_n = \begin{bmatrix} x_n & 0 & \cdots & 0 \end{bmatrix}^T$. Note that the time index, $n+1$, in the first equation of (18) is substituted for n of (17) to implement the Kalman filter. Hereafter, the coefficient of the AR process is referred to as a fading parameter.

Let $\hat{\mathbf{h}}_{n+1}$ denote the estimate of $\mathbf{h}_n$ given the observations $\{r_i\}$ the sample time from 0 to n. Then, through the Kalman filter, the channel estimate $\hat{\mathbf{h}}_{n+1}$ can be obtained by a set of recursions. First, channel estimation is based on the previous system state.

$$\hat{\mathbf{h}}_{n+1|n} = \mathbf{F}_n \hat{\mathbf{h}}_n \tag{19}$$

The error covariance matrix is predicted as

$$\mathbf{P}_{n+1|n} = \mathbf{F}_n \mathbf{P}_n \mathbf{F}_n^T + \mathbf{Q}_{n+1} \tag{20}$$

According to the new observations to amend the first step of the estimate, resulting in a new estimate, the new estimation error is

$$e_{n+1} = r_{n+1} - \hat{r}_{n+1} = r_{n+1} - \mathbf{x}_{n+1}^T \hat{\mathbf{h}}_{n+1|n} \tag{21}$$

An improved state estimate is given based on the estimation error.

$$\hat{\mathbf{h}}_{n+1} = \hat{\mathbf{h}}_{n+1|n} + \mathbf{k}_n e_n \tag{22}$$

$$\mathbf{P}_{n+1} = \mathbf{P}_{n+1|n} - \mathbf{k}_{n+1} \mathbf{x}_{n+1} \mathbf{P}_{n+1|n} \tag{23}$$

where, $\mathbf{k}_{n+1}$ is kalman gain, can be expressed as

$$\mathbf{k}_{n+1} = \mathbf{P}_{n+1|n} \mathbf{x}_{n+1}^* \left(N_0 + \mathbf{x}_{n+1}^T \mathbf{P}_{n+1|n} \mathbf{x}_{n+1}^* \right)^{-1} \tag{24}$$

It should be noted that the state vector and the error covariance matrix are initially assigned to zero vector and identity matrix, respectively; that is, $\hat{\mathbf{h}}_{0|0} = \mathbf{0}$, $\mathbf{P}_{0|0} = \mathbf{I}_p$.

When the Doppler rate $f_d T$ is available at the eceiver, the AR parameters a_i and the correlation matrix Q_{n+1} of the process noise v can be computed by solving the so-called Yule-Walker (YW) equations[13].

$$a = J_0 \left(2\pi f_d T \right) \tag{25}$$

$$Q_{n+1} = \left(1 - a^2 \right) \sigma_h^2 \left(n + 1 \right) \tag{26}$$

IV. SIMULATION RESULTS

In this section, we carry out a comparative study on the estimation performance of FBMC/OQAM in fast fading channel implementing the proposed Kalman filter channel estimate algorithm based on feedback interference pilot, traditional comb pilot LS channel estimation, feedback interference calculation pilot LS channel estimation and Kalman filter channel estimate algorithm based on traditional comb pilot.

In order to study the performance of time-varying channel estimation based on pilot kalman filtering in multipath fading channels, in all simulations, a Rayleigh multipath channel is adopted, with the multipath delay as (0 1 2 3 4)T_s, where T_s represents the sampling time, and the fading of each path as (-2.748 -4.413 -11.052 -18.500 -18.276)dB. In all simulations, no channel coding is added. The remaining simulation parameters are shown in the table II.

TABLE II
SIMULATION PARAMETERS

Subcarrier spacing	10.94kHz
Sampling frequency	11.2MHz
Carrier frequency	3.5GHz
Subcarrier number	1024
System bandwidth	10MHz
Baseband modulation order of OQAM	4
Overlap factor	4
Time domain interval of the pilot distribution	8
Frequency domain interval of the pilot distribution	4
Channel estimation	LS
Interpolation method	linear interpolation

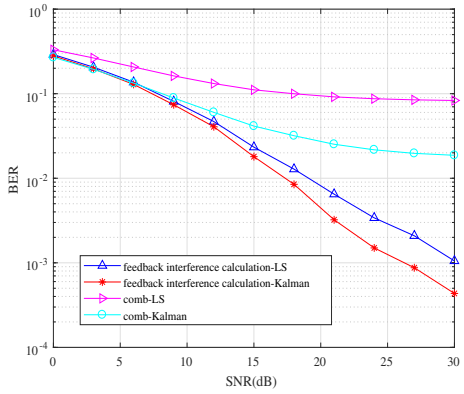

Fig. 6. Comparison of BER of LS and Kalman filter channel estimate algorithms at 50km/h

In order to verify the superiority of channel estimation of Kalman filter based on feedback interference calculation pilot in time-varying multipath channel, Fig.6 shows the performance comparison at the speed on 50km/h. It is obvious that Kalman filter method compared with the traditional LS, Kalman filter performance improved significantly, mainly

because Kalman filter can better track the channel changes. It can also be seen that the performance of the Kalman filtering method based on the feedback interference calculation pilot is better than the traditional comb-based Kalman filtering method. This is because the feedback interference calculation pilot utilizes the internal interference of the FBMC and reduces the error caused by the internal interference to the channel estimation.

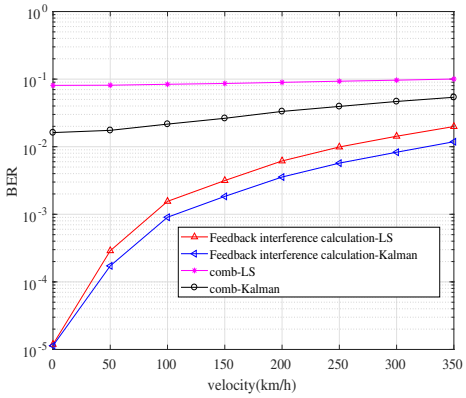

Fig. 7. The performance comparison at different speeds

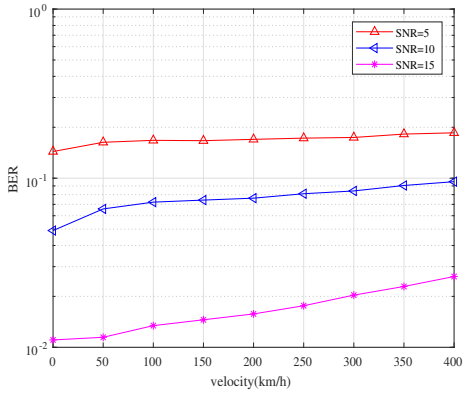

Fig. 8. Performance of Kalman Filter Based on Feedback Interference Calculation Pilot at Different SNRs

Fig.7 shows the performance comparison at different speeds. It is clear that as the speed increases, that is, the Doppler shift increases, the bit error rate also increases. The Kalman filter based on the feedback interference calculation pilot has better performance than the other three channel estimation algorithms. When the speed is zero, that is, there is no Doppler shift, the performance of the feedback interference calculation algorithm is not much different from the Kalman filter algorithm based on the feedback interference calculation pilot, because the feedback interference calculation pilot calculates the internal interference, feedback interference calculation algorithm for channel tracking and kalman filtering compared has no big difference. This confirms that a Kalman filter estimator based on feedback interference calculation pilots can utilize fading channel statistics and be able to track fast changes in rapidly changing fading channels.

Fig.8 is the simulation of the bit error rate obtained by the Kalman filter estimation algorithm based on the feedback interference calculation pilot under different signal-to-noise ratios. It is clear that as the speed increases, the BER presents an increasing trend at the same SNR and the BER under different SNR shows different growth trend.

V. CONCLUSIONS

Based on the FBMC/OQAM system for time-varying channel estimation, this paper proposes a Kalman filter based on feedback interference calculation pilot. The notable feature of this method is that it has good performance in time-varying multipath channels. Meanwhile, a method of detecting the state changes is proposed according to the related changes of channels. After the theoretical proof and simulation test, it shows that the proposed Kalman filtering method has better results for time-varying multipath channel estimation compared with the existing algorithms.

ACKNOWLEDGMENT

This research was supported by the National Science Foundation of China (Under Grant: 61671173).

REFERENCES

[1] G. Wunder, P. Jung, M. Kasparick, and T. Wild, "5GNOW: non-orthogonal, asynchronous waveforms for future mobile applications," *Communications Magazine IEEE*, vol. 52, no. 2, pp. 97–105, 2014.

[2] D. M. Arndt and C. A. F. D. Rocha, "Performance comparison between OFDM and FBMC systems in Digital TV transmission," in *Communications*, 2011, pp. 1–6.

[3] J. B. Dor, V. Berg, and D. Ktenas, "Performance of FBMC Multiple Access for relaxed synchronization cellular networks," in *GLOBECOM Workshops*, 2015, pp. 983–988.

[4] H. Saeedi-Sourck, S. Sadri, Y. Wu, and B. Farhang-Boroujeny, "Near Maximum Likelihood Synchronization for Filter Bank Multicarrier Systems," *IEEE Wireless Communications Letters*, vol. 2, no. 2, pp. 235–238, 2013.

[5] J. P. Javaudin, D. Lacroix, and A. Rouxel, "Pilot-aided channel estimation for OFDM/OQAM," in *Vehicular Technology Conference, 2003. Vtc 2003-Spring. the IEEE Semi*, 2003, pp. 1581–1585 vol.3.

[6] W. Cui, D. Qu, T. Jiang, and B. Farhang-Boroujeny, "Coded Auxiliary Pilots for Channel Estimation in FBMC-OQAM Systems," *IEEE Transactions on Vehicular Technology*, vol. 65, no. 5, pp. 2936–2946, 2016.

[7] J. M. Choi, Y. Oh, H. Lee, and J. S. Seo, "Pilot-Aided Channel Estimation Utilizing Intrinsic Interference for FBMC/OQAM Systems," *IEEE Transactions on Broadcasting*, vol. PP, no. 99, pp. 1–12, 2017.

[8] J. Bazzi, P. Weitkemper, and K. Kusume, "Power Efficient Scattered Pilot Channel Estimation for FBMC/OQAM," in *SCC 2015; International Itg Conference on Systems, Communications and Coding; Proceedings of*, 2015, pp. 1–6.

[9] C. Hao, S. Wu, X. Liu, and K. Ma, "A New Type of Comb Pilot in FBMC/OQAM," *IEEE WCNC 2018 accept*.

[10] C. Ll, J.-P. Javaudin, R. Legouable, A. Skrzypczak, and P. Siohan, "Channel estimation methods for preamblebased OFDM/OQAM modulations," *European Transactions on Telecommunications*, vol. 19, no. 7, pp. 741–750, 2010.

[11] M. G. Bellanger, "Specification and design of a prototype filter for filter bank based multicarrier transmission," in *IEEE International Conference on Acoustics, Speech, and Signal Processing, 2001. Proceedings*, 2001, pp. 2417–2420 vol.4.

[12] K. E. Baddour and N. C. Beaulieu, "Autoregressive modeling for fading channel simulation," *IEEE Transactions on Wireless Communications*, vol. 4, no. 4, pp. 1650–1662, 2005.

[13] B. Porat, *Digital processing of random signals: theory and methods*. Prentice Hall Inc, 1994.